

## PHOTO-OXIDATION OF THERMALLY EVAPORATED $\text{As}_2\text{S}_3$ THIN FILMS

P. J. Allen\*, B. R. Johnson, B. J. Riley

Pacific Northwest National Laboratory, Richland, WA USA

Photo-oxidation of arsenic trisulfide is the process whereby the surface of  $\text{As}_2\text{S}_3$  glass is chemically altered and degraded due to exposure to light in the presence of water vapor. For as-deposited, thermally evaporated,  $\text{As}_2\text{S}_3$  thin films the degradation process and the subsequent products formed vary as a function of incident wavelength. This process was studied by exposing as-deposited thin films to six different wavelengths from 380 to 525 nm in a controlled temperature and humidity environment. Scanning electron microscopy (SEM), energy dispersive spectroscopy (EDS), and x-ray diffraction (XRD) were used to characterize the thin films before and after exposure. At wavelengths less than 428 nm, crystalline arsenolite ( $\text{As}_2\text{O}_3$ ) formed on the surface, with only minor modification of the short-range molecular structure of the film. At longer wavelengths, the short range order of the film was altered from the as-deposited state to that typical of thermal annealing. A mechanism to explain these processes is proposed.

(Received July 4, 2005; accepted July 21, 2005)

*Keywords:*  $\text{As}_2\text{S}_3$ , Thin film, Photo-oxidation, SEM, EDX, XRD,  $\text{As}_2\text{O}_3$

### 1. Introduction

The ability to locally photoinduce optical index change and volume expansion has encouraged extensive study of the chalcogenide glass family. Fabrication of microlenses, diffraction gratings, and waveguides via laser exposure have been reported [1-5]. A host of high purity glasses from this family provide excellent transmission in the infrared [6]. These properties make feasible not only new telecom application but integrated optics that can support spectroscopy systems operating from 3 to 12  $\mu\text{m}$ .

Material stability is important for any photonic component. Two known instabilities in  $\text{As}_2\text{S}_3$  films are the formation of surface oxides and the presence of metastable realgar in the films. Thorough understanding of what conditions cause corrosion and material relaxation is necessary before  $\text{As}_2\text{S}_3$  can be used for photonic components.

The aim of this paper is to report on the correlation of corrosive attack on thermally evaporated  $\text{As}_2\text{S}_3$  thin films with environmental conditions. Researchers have reported photo-oxidation, or lack of it, under various conditions [7-12]. We have further pursued this topic by examining the wavelength dependence of oxide formation. Additionally, photodarkening appears to play a role in the corrosion.

### 2. Experimental procedure

Fused quartz slides were cleaned by acid etching in 5%HF:5% $\text{HNO}_3$ :90%DIW (18.2  $\text{M}\Omega\text{-cm}$ ), by volume, for 20 minutes, rinsed with deionized water (DIW) and heated to 1000  $^\circ\text{C}$  for one hour in a Thermolyne 79400 furnace, with a fused quartz tube interlining, to remove surface hydrocarbons [13]. Commercially obtained bulk  $\text{As}_2\text{S}_3$  glass (Amorphous Materials, Inc.) was heated to  $320 \pm 1^\circ\text{C}$  at  $10^{-6}$  Torr and deposited onto the quartz substrates at 6-8  $\text{\AA}/\text{s}$  to achieve

---

\* Corresponding author: Paul.Allen@pnl.gov

2  $\mu\text{m}$  thick films. The substrate holder was unheated while double planetary motion helped achieve thickness variation below 1%. Stoichiometry of the films was verified to be within  $\pm 2$  atomic % of the bulk material using SEM/EDS.

Five samples were prepared to evaluate the effects of thermal annealing on the molecular structure of the films. Four samples were ramped from room temperature to 110, 130, 150, or 170  $^{\circ}\text{C}$  at 1  $^{\circ}\text{C}$  per minute, soaked for two hours, and cooled to room temperature at the same rate. The annealing was done in an evacuated chamber. One sample was not annealed.

To provide wavelength specific optical exposure six LEDs (Fig. 1) with wavelengths centered at 380, 405, 428, 470, 507, and 525 nm were used to illuminate the samples. Every sample was illuminated by a single LED with a  $30^{\circ}$  cone, 5 mm from the film, with  $0.35 \pm 0.02$  mW of optical power. All samples were placed in an environmental chamber held at  $50 \pm 1^{\circ}\text{C}$  and  $80 \pm 5\%$  relative humidity for fourteen days. Samples are referenced by the value of their peak illumination wavelength.

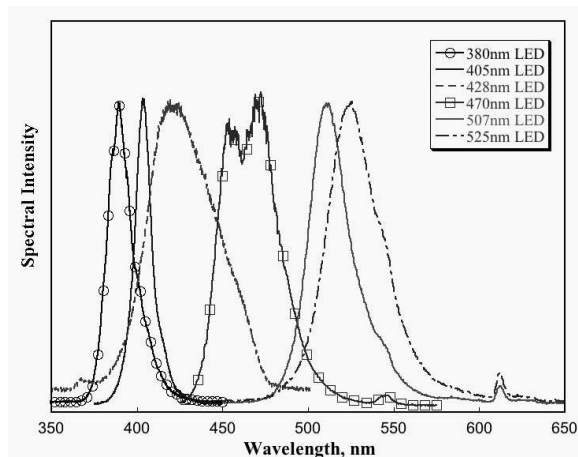


Fig. 1. Spectral intensity of LEDs.

X-ray diffraction measurements were performed with a Scintag PAD V diffractometer using  $\text{Cu K}\alpha$  radiation (40 kV and 40 mA) and equipped with a Peltier-cooled charge coupled device detector. The experiments were done using  $\theta - 2\theta$  geometry in a step-scan approach from  $5^{\circ}$  to  $70^{\circ}$   $2\theta$  with a step size of  $0.04^{\circ}$   $2\theta$ , and a dwell time of 6 seconds per step. Each sample was loaded into a Scintag 12-position automatic sample changer. Jade 6 $\text{\textcircled{R}}$  software was used analyze the spectra for the presence of arsenolite ( $\text{As}_2\text{O}_3$ ), and to characterize the shape of the different amorphous humps due to the substrate (fused quartz –  $\text{SiO}_2$ ), realgar ( $\text{As}_4\text{S}_4$ ), and orpiment ( $\text{As}_2\text{S}_3$ ). Since these samples were thin films and the arsenolite crystals were growing along a single, planar surface, the orientation of these crystals on the planar surface was not random. Due to their faceted nature, the crystals tended to grow in an oriented manner. Since it was not feasible (or desirable) to prepare a powder sample with random orientation due to the small sample volume, a user file was created to facilitate comparison of the samples to each another.

### 3. Results

XRD spectra of as-deposited and thermally annealed films are shown in Fig. 2. To enhance comparison of these spectra the intensities of each spectrum has a fixed offset, i.e. the spectra are stacked above one another. This spectral series is of interest for comparison to those of the illuminated samples. A feature of interest in this series is near  $16^{\circ}$   $2\theta$ , which corresponds to the realgar signature (Fig. 6A). As the annealing temperature is increased (Fig. 2) this realgar peak decreases. At the same time a peak at  $18^{\circ}$   $2\theta$  appears, which is explained by the presence of orpiment (Fig. 6B). These intensity changes are partially obscured by the quartz signature.

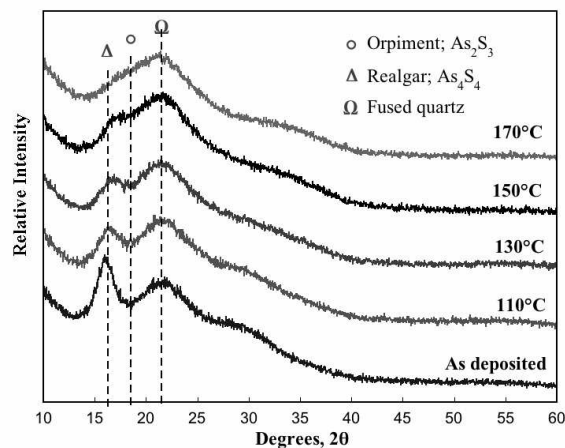


Fig. 2. XRD spectra for  $\text{As}_2\text{S}_3$  thin films on fused quartz substrates thermally annealed at different temperatures.

XRD was also performed on the illuminated samples after fourteen days in the environmental chamber (Fig. 3). The sharp peaks from samples 308 and 405 at  $14^\circ$ ,  $28^\circ$ , and  $35.5^\circ$   $2\theta$  correlate with the spectra of arsenolite. Note that the spectra of samples 428 to 525 are free of these peaks. Spectra from samples 380 and 405 also retained the peak at  $16^\circ$   $2\theta$  that was present in the as-deposited films and again indicates the presence of realgar. As in the thermally annealed series, the realgar feature decreases while the orpiment peak increases, the difference in this case is this series follows increased wavelength exposure instead of increased temperature.

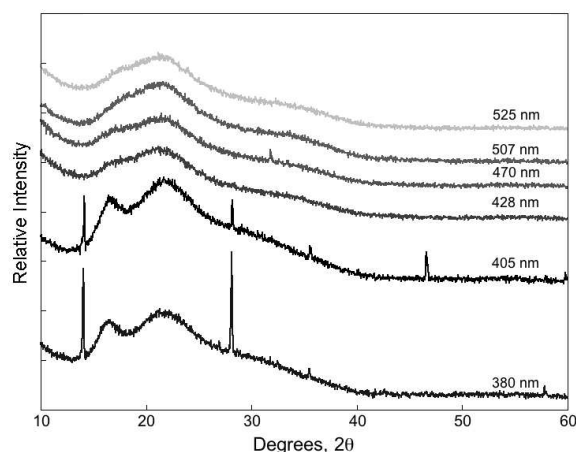


Fig. 3. XRD spectra of as-deposited  $\text{As}_2\text{S}_3$  thin films exposed to as-labeled wavelengths at  $50^\circ\text{C}$  and 80% RH for 14 days.

SEM micrographs in Fig. 4 were collected from samples 380 and 525 after XRD measurement. These micrographs show the contrast between an unilluminated region of sample 380 (Fig. 4A) and an area subject to direct illumination by the 380 nm LED (Fig. 4B). The large structure in Fig. 4B is an arsenolite crystal. Additionally, the film's surface has acquired a textured appearance. The illuminated region of sample 525 (Fig. 4C) shows no response to its environment, the 525 nm LED caused no discernable degradation to the film.

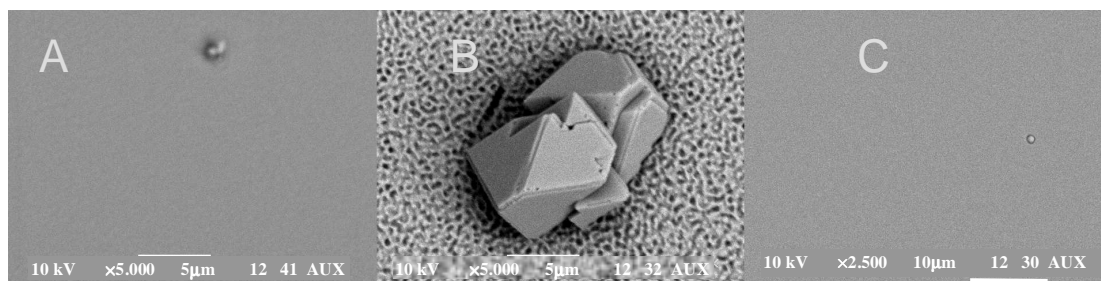


Fig. 4. SEM micrographs of films subjected to fourteen days in the environmental chamber. (A) Sample 380, unexposed region (B) Sample 380, exposed region (C) sample 525, exposed region.

## 4. Discussion

### Structural effects of thermal annealing

XRD analysis of as-deposited and thermally annealed films is shown in Fig. 2. Close examination of the spectra revealed that thermal annealing created a change in the short-range order of the film. The as-deposited thin films have a short-range order that indicates the presence of  $\text{As}_4\text{S}_4$  moieties in the film [14]. This is consistent with what is known from Raman investigation of vaporized  $\text{As}_2\text{S}_3$ ; it dissociates into  $\text{As}_4\text{S}_4$  and excess sulfur [15]. Additionally, Raman spectra of as-deposited films indicates the presence of homopolar bonding (e.g. As-As and S-S bonds) which is characteristic of  $\text{As}_4\text{S}_4$  (Fig. 5) [14]. Thus, one can conclude that one result of thermal annealing is to homogenize the  $\text{As}_4\text{S}_4$  and excess sulfur in the film such that the short-range order is representative of a random, distributed network of orpiment (Fig. 6B). Mechanistically, this involves breaking the As-As bonds in the  $\text{As}_4\text{S}_4$  moieties and forming As-S<sub>3</sub> pyramidal units that link to form 12-membered ring structures of hetero-polar As-S bonds.

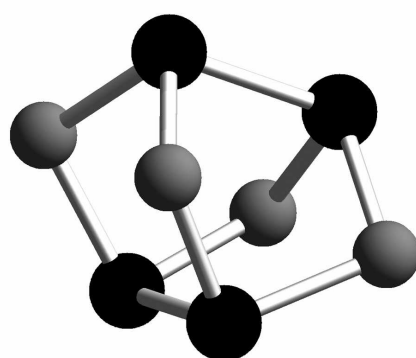


Fig. 5. Crystal model of realgar,  $\text{As}_4\text{S}_4$ .

### Photo-oxidation of as-deposited, unannealed thin films

The most interesting result from this photo-oxidation study was the varied response of the films by wavelength. At wavelengths less than 428 nm the short-range order, realgar-like, structure of the films remained essentially unaltered while a significant amount of arsenolite formed on the surface (Fig. 3, Fig. 4). Above 428 nm the structure of the films was altered such that they had a random distributed network of orpiment, similar to that formed after thermally annealing the films (Fig. 2, Fig. 3). Surprisingly, though the structure of the film was altered, there was no evidence of corrosive attack at these longer wavelengths based on XRD or SEM investigations.

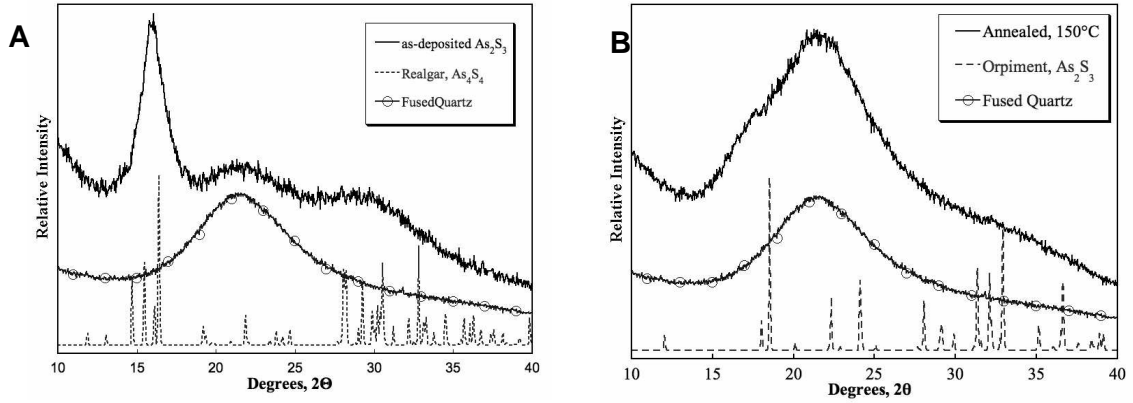
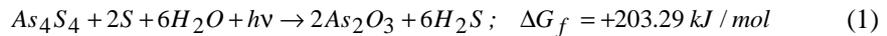


Fig. 6. XRD spectra of thermally evaporated As<sub>2</sub>S<sub>3</sub> thin films (A) as-deposited and (B) thermally annealed at 150 °C.

Two main causes for the variation in photo-oxidation with wavelength are proposed. First, since the photo-oxidation was observed only at the higher photon energies it implies that there may be some minimum activation energy necessary for the reaction to occur. Second, the absorptivity of As<sub>2</sub>S<sub>3</sub> increases sharply below 600 nm; the penetration depth is less than 170 nm below 428 nm [17]. Consequently, at wavelengths below 428 nm (>2.90 eV) all of the optical energy was deposited at the near-surface of the films (Fig. 7) where there was adsorbed water from the humid environment. This reaction can be described as:



The energy required for reaction (1) to occur is 2.11 eV (586 nm). Since the observed threshold energy for photo-oxidation was greater than 2.90 eV, it can be concluded that an additional activation energy is required for the reaction to occur. One thought is that the process is dependant upon the photo-dissociation of water. However, the energy required for photo-dissociation of an isolated gaseous water molecule (e.g. remove one hydrogen atom) is 5.16 eV (240 nm) [16], thus this is not a likely reaction mechanism. More likely, the water present would be in a liquid phase on the surface of the film. Liquid water spontaneously dissociates into hydroxyl and hydronium ions via the pH equilibrium, thereby lowering the energy required to manipulate bonds for reaction (1) to occur.

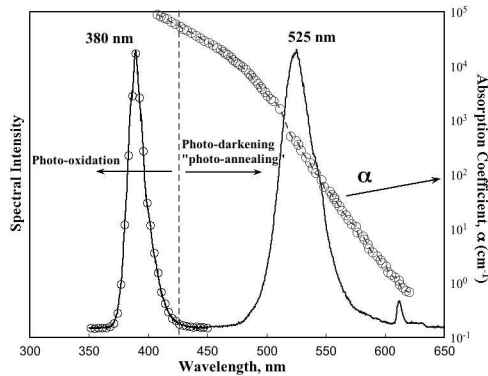
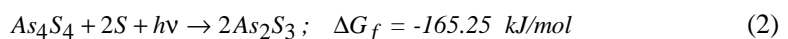


Fig. 7. Spectral intensities for the 380 and 525 nm LEDs. Overlaid on this plot is the absorption coefficient versus wavelength.

The following equation (2) is a proposed photo-chemical reaction to describe the changes in molecular structure observed in thin films exposed to wavelengths longer than 428 nm:



There is a sufficient energy release for this reaction to occur spontaneously but apparently the kinetics specific to an amorphous solid retard this reaction. Only modest energy was required to initiate this reaction (e.g. < 2.9 eV) and promote the homogenization of the thin film.

In both reactions, we propose that the primary re-active component of the as-deposited thin films is the As-As bond present in the realgar moieties (Fig. 5), and that this bond is susceptible to manipulation by absorbed photons. At higher energies (shorter wavelengths) all of the energy is deposited on the surface of the “opaque” film at the interface with the adsorbed water layer. When the As-As bond is broken by the incident photons, hydroxyl ions from equilibrium dissociation of water are present and facilitate the formation of arsenolite. At lower energies (longer wavelengths) close to the absorption edge, the incident photons penetrate deeper into the body of the film. In this case, when the As-As bond is broken, residual sulfur is present, and due to the favorable thermodynamics, the  $\text{As}_4\text{S}_4$  moieties convert to form a randomly distributed amorphous orpiment structure.

## 5. Conclusion

Photo-oxidation occurred on as-deposited thin films of  $\text{As}_2\text{S}_3$  only when exposed to wavelengths less than 428 nm and in the presence of humidity. At wavelengths longer than 428 nm the short-range order (molecular structure) of the thin film was modified via photodarkening such that it had the same XRD spectra as that produced by thermal annealing. Such alteration of the short-range structure of the films did not occur below 428 nm. The wavelength distinction between photo-oxidation and “photoannealing” is postulated to be due to two different effects. First, a critical activation energy associated with the formation of the corrosion products. Second, the correlation between the absorption coefficient of  $\text{As}_2\text{S}_3$  and the transition between the two phenomena.

Future work could include investigating the specifics of the activation energy and more extensive comparisons of photoannealing versus thermal annealing.

## Acknowledgements

Funding was provided by the U. S. Department of Energy’s (DOE) National Nuclear Security Administration (NNSA/NA-22) Office of Nonproliferation Research and Engineering; DARPA’s Laser Photoacoustic Spectroscopy (LPAS); and the Pacific Northwest National Laboratory (PNNL), operated for the DOE by Battelle under Contract DE-AC05-76RL01830. The authors would like to express their gratitude to John Schultz, Norm Anheier, S. K. Sundaram, Nicolas Ho, James Martinez, Kannan Krishnaswami, and Jarrod Crum of PNNL, for their contribution and consultation on this project.

## References

- [1] A. Zakery, P. J. S. Ewen, A. E. Owen, *Journal of Non-Crystalline Solids*. **198-200**, 769-773 (1996).
- [2] J.-F. Viens, C. Meneghini, A. Villeneuve, T. V. Galstian, E. J. Knystautas, M. A. Duguay, K. A. Richardson, T. Cardinal, *Journal of Lightwave Technology* **17**(7), 1184-1191 (1999).
- [3] A. V. Rode, *Applied Surface Science* **197-198**, 481-485 (2002).
- [4] N. C. Anheier, B. R. Johnson, S. K. Sundaram, *Non-Crystalline Materials for Optoelectronics*. 2004. Bucharest: INOE Publishing House.
- [5] H. Hisakuni, K. Tanaka, *Optical Fabrication of Microlenses in Chalcogenide Glasses*, *Optics Letters* **20**(9), 958-960 (1995).
- [6] J. Lucas, *Infrared glasses*. *Current Opinion in Solid State & Materials Science* **4**(2), 181-7 (1999).
- [7] E. Marquez, J. M. Gonzalez-Leal, R. Jimenez-Garay, M. Vlcek, *Thin Solid Films* **396**(1-2), 183-190 (2001).
- [8] A. J. Apling, M. F. Daniel, A. J. Leadbetter, *Thin Solid Films* **27**(2), L11-L13 (1975).
- [9] K. Petkov, V. Krastev, T. Marinova, *Surface & Interface Analysis* **22**(1), 202-205 (1994).
- [10] P. J. Allen, B. R. Johnson, R. T. Baran, N. C. Anheier, S. K. Sundaram, M. H. Engelhard, B. T. Broocks, *Glass & Optical Materials Division Fall 2004 Meeting*. 2004, Cape Canaveral, Florida USA.
- [11] Berkes, *Journal of Applied Physics* **42**(12), (1971).
- [12] S. Seal, *Corrosion* **59**(2) (2003).
- [13] B. G. Aitken, C. W. Ponader, *Journal of Non-Crystalline Solids* **274**(1), 124-130 (2000).
- [14] M. L. Slade, R. Zallen, *Solid State Communication* **30**, 357-360 (1979).
- [15] R. J. Nemanich, G. A. N. Connell, T. M. Hayes, R. A. Street, *Thermally Induced Effects in Evaporated Chalcogenide Films I. Structure*. *Physical Review B*, **18**(12), 6900-6914 (1978).
- [16] *CRC Handbook of Chemistry and Physics*, ed. D. R. Lide. Vol. 85, 2005.
- [17] K. Zallen, *The physics of amorphous solids*. 1983: John Wiley & Sons.